Computational and experimental analysis of particulate distribution during Al–SiC MMC fabrication

S. Naher, D. Brabazon, L. Looney

Materials Processing Research Centre, Mechanical and Manufacturing, Dublin City University, Collins Avenue, Glasnevin, Dublin 9, Ireland.

Abstract

There are many factors which influence the incorporation of particulate in metal matrix composites (MMCs). This paper presents work which examines the effect of viscosity during Al–SiC MMC production. Processing periods (up to 65 min), stirring speeds (50– 500 rpm), and re-inforcement sizes (13–100 lm) for two different viscosity levels (1 and 300 mPa s) were investigated. Computer simulations, room temperature analogue fluid simulations, and MMC castings were performed. Volume fraction results of SiC at different locations within the fluids were assessed by each of these methods and compared. From these tests, a stirring speed of 200 rpm for the lower viscosity fluid and 300 rpm for the higher viscosity fluid were found to be best in order to produce uniform distributions of SiC. In order to obtain a uniform re-inforcement distribution in the lower viscosity system, stirring periods were found to range from 14 to 170 s and for the higher viscosity system from 540 to more than 3920 s. Fully uniform suspensions remained for just a couple of seconds in the lower viscosity system compared to about an hour for the higher viscosity system. The modelling approach chosen was found to be useful in predicting settling behaviour in the semi-solid metal.

1. Introduction

In a recent review, it was shown that metal matrix composites (MMCs) can be used in a wide cross-section of applications ranging from civil structures, to aerospace, to recreational products [1]. This is due to the capability of MMCs to be designed to provide a vast array of mechanical, thermal and dimensional accuracy properties. This same review presented a number of the methods by which MMCs can be fabricated. In order to produce homogeneously reinforced MMC components, the method chosen for particle incorporation within the matrix is important. Some techniques for introducing and mixing the particles have inherent disadvantages. Gas injection of particles, for example, may result in part porosity and sophisticated techniques using combined ultrasonic transduction in the centrifugal casting process can lead to undesirable variations in the percentage of particles from the inner to outer part of a billet [2]. Other techniques such as squeeze casting and powder metallurgy methods have enabled high fractions of reinforcement to be incorporated in the final casting [3,4]. In comparison, compocasting is a relatively simple process of mechanical agitation for the production of MMC which can be easily

scaled as required [5]. This process involves the addition of particulate reinforcement into semi-solid metal (SSM) either before or during agitation of the fluid. Previous work has analysed the damage mechanisms in alumina reinforced wrought aluminium composites [6]. This work has shown that composites produced by the stir casting route can be further processed by thixoforging to obtain good mechanical properties. Similar benefits in the mechanical properties of reinforced thixocast aluminium alloys were also noted with proper selection of heat treatments [7]. The latter two references have in particular shown that with stir cast feedstock and appropriate processing conditions thixo-formed MMC components can be produced for aerospace applications.

The clustering of the particulate reinforcement during MMC production has an important influence on MMC properties. This is undesirable as it leads to nonhomogeneous response and lower macroscopic mechanical proper-ties. Particle clustering can occur due to chemical binding, reduction of surface energy, or segregation of the particles [8]. As would be expected, heavy particles settle more quickly [9-11]. For similar reasons, clustering is also a contributory factor to the reinforcement settling more quickly [8,12]. In recent work by Prabu et al., it was noted that particle clustering occurred at a stirring speed of 500 rpm during the stir cast production of aluminium alloy A384 with 10% of 64 μn sized SiC reinforcement [13]. In this case, the long elevated pre-heating of the SiC particles may have contributed to chemical bonding between the particles [8]. At higher speeds were the surface layer may have broken down, the authors noted that no particle clustering occu-red. In cases where particle clustering does not occur, the interaction of particles with each other at higher volume fractions can cause reduced particle settling rates [11]. Another factor that may lead to particle segregation is particle pushing by the solidification front. If a high enough solidification front speed is developed, called the critical speed, the particles are engulfed rather than pushed. A review of the critical velocity models has recently been presented by Youssef et al. [8]. As the particulate size (or cluster size) increases the critical velocity reduces. This is noted as being due to the reduction in interfacial energy difference between the particle and the advancing solid/liquid front as the particulate size increases.

In order to fabricate MMCs with good mechanical properties, other important factors that need to be considered include the effect of poor reinforcement wettability by the matrix and the propensity for the introduction of porosity during the particle incorporation phase [14]. With appropriate choice of materials, fast but non-turbulent agitation, inert atmospheres, and laminar direct flow path die filling methods these latter problems can largely be over-come [15]. However, lack of knowledge of the flow field remains one of the main problems for homogeneous MMC production. If process parameters are not adequately controlled non-homogeneous particle distribution can arise due to insufficient particulate dispersion, sedimentation, solid front particle pushing or flow generated segregation [16]. This in turn results in generally undesirable non-uniform MMC properties.

Developing predictive models for the flow fields and resulting particulate distribution can be a complex process. In the compocasting process, selection of stirring speed and period is essential for the effective incorporation of particles to occur [17]. In addition, the stirrer/vessel geometry, melt temperature, and the material type, amount and nature (e.g. fibrous, faceted, or size) of the particles are some of the main factors to consider when develoing these models [18-21]. The important influence of stirrer height, blade angle and type on particle distribution has been examined in past studies [22,23]. Previous work has also investigated the minimum agitation speed that will result in a uniform suspension of particles with a view to avoiding turbulent flow and porosity development [18]. Other workers have used transparent moulds to obtain visual data from the composite production process to aid model development [24]. These previous computational models of MMC production generally take some account of the viscosity variations in the semi-solid fluid. Viscosity changes with volume fraction, shape, and size of the reinforcing phase. The viscosity is also dependent on the shear rate, stirring time and cooling rate [25]. Most numerical models of suspension flow use an effective viscosity value based on a function of the solid content and shear rate. For example, Stoke's law, with such viscosity values, can be applied to predict particle dispersion or settling rate [26]. Knowledge of the dispersion and settling rates allows the cast house to deter-mine, respectively, the time period required to produce a homogeneous distribution of reinforcement and how long a prepared batch of MMC can be held before it needs to be processed. This paper presents work focused on the determination of the re-enforcement dispersion and settling times which influence the production of MMCs. Computational models of the flow fields for these processes in analogue systems were developed to gain more in depth understanding.

2. Experimental

The computational models were built as two-phase fluid flow models. The first phase was set as either a water or glycerol/water mixture and the second phase as 10% volume fraction of SiC particulate. At the start of these simulations the 10% SiC was positioned at the base of the mixing vessel with a packing volume of 0.6. A particle size of 13 μm was used in most of the tests, however, particles of 30 and 100 μm in size were also investigated to deter-mine their effect on settling rate. These phases were chosen as they enabled a Newtonian computational model to be applied and room temperature analogue experimental test comparisons. The viscosity behaviour of liquid aluminium has been recorded by many workers as Newtonian with a viscosity value, similar to water, of 1 mPa s. At very low shear rates ($<2\ s^{-1}$) and for periods of up to at least 8 min, the viscosity of semi-solid aluminium alloy at 0.3 fraction solid can be approximated at 300 mPa s [27]. These previous results indicate that for very low shear rate situations, such as during particulate settling, the normally thixotropic semi-solid metal can be approximated as a Newtonian fluid for modelling purposes. These values were also set as viscosities of the analogue fluids, water and glycerol/water, respectively.Water, glycerol and SiC densities were set at 1000, 1260, and 3210 kg/m^3, respectively.

The physical dimensions of the modelled system were set to those of a flat-bottomed cylindrical crucible of 105 mm inner diameter. The crucible was filled in all tests to a level of 65 mm. A 80 mm diameter steel four flat bladed impel-ler, with 10 mm wide and 2 mm thick blades set at 45° to the vertical, was arranged to pump in the upwards direc-tion. A thin coating of boron nitride was applied to the impeller to avoid contamination of the melt and prevent corrosion of the stirrer. The stirrer height in all tests was 20 mm from the base of the crucible. In order to aid com-parison of results, these model settings indicated above were identical to those used in the analogue and MMC fab-rication experimental work. Appropriate processing peri-ods and stirring speeds for the experimental tests were informed from the results of the computational models. Further specific details on the modelling, analogue and MMC fabrication experiments are given below.

2.1. Computational models

The computational fluid dynamic (CFD) models used in this work were developed in Fluent Version 4.5 and add on package Mixsim. Initial velocity distributions along the stirrer blade for this model were obtained from a 3D velocity model of the flow at the investigated stirring velocities (50, 100, 150, 200, 250, 300, 400, and 500 rpm). The initial velocity profiles obtained from the 3D simulations, which showed that the flow inside the crucible was symmetrical about the impeller axis, were used in 2D simulations to determine the evolution of flow parameters over longer time periods. Velocity components, kinetic energy dissipation, eddy dissipation, and the volume percentage of SiC measurements were taken through the vessel at different times after the commencement of stirring. From initial trials and Reynolds number examination, the k — € turbulent model was chosen to model the water system and the laminar flow model for the glycerol/water system. Axisymmetric multiphase time dependent Eulerian (granular) models were used. All of the measurements reported here were taken along the vertical plane mid way between the impeller blades. This is represented in Fig. la as plane AA. The three directions of measurement were axial, x, radial, r, and circumferential, 0. The height positions at which measurements were taken in the crucible are indicated in Fig. 1b.

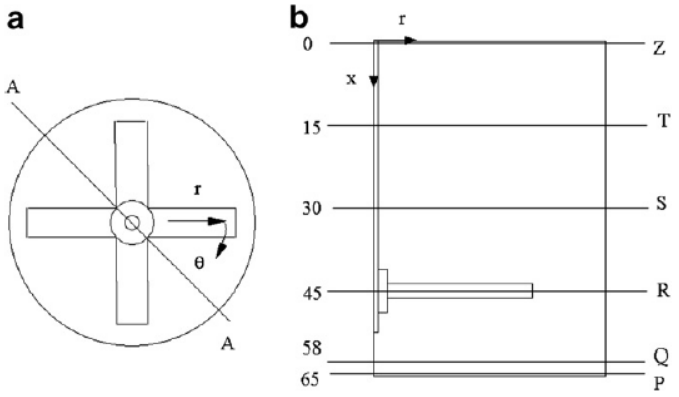

Fig. 1. Positions at which measurements were taken in the mixing crucible; (a) represents the plan view and (b) the elevation on A–A. Positions Z and P are at the top of the fluid surface and the base of the crucible, respectively. Positions T, S, and R are 15 mm, 30 mm, and 45 mm below the fluid surface, respectively.

2.2. Room temperature analogue testing

In the analogue experiments, water and glycerol/water solution were used to simulate liquid and semi-solid aluminium, respectively. A glycerol/water solution with a viscosity of 300 mPa s, similar to that encountered at 0.3 fraction solid in the processing of SSM, was used [27,28]. Accurate fluid viscosity control was ensured by using a cone and plate viscometer (Rheological International, model no. RI:2:L). The same SiC reinforcement particulate as used in the modelling and MMC fabrication tests was used in these tests. At the start of testing the 10% SiC particles were at the bottom of a flat bottomed transparent glass crucible with dimensions as indicated above. A speed controlled DC motor enabled accurate control of the stirring speed between 50 and 500 rpm [23]. A uniform dispersion of SiC throughout the liquid was produced by means of mechanical shearing with the same type of four flat bladed stirrer as used in the modelling and MMC fabrication experiments. Dispersion times were judged visually by eye. To examine settling rates, a uniform dispersion of SiC was produced throughout the fluids by means of mechanical shearing at 200, 300, and 500 rpm. When shear-ing was stopped, settling times for the uniformly dispersed particles in the different fluids were measured.

2.3. MMC fabrication

The compocaster was made in-house and is shown schematically in Fig. 2. A screw driven actuator was bolted vertically beneath the compocaster. The crucible was mounted on a ceramic spacer which was in turn attached to the actuator end plate. This arrangement allowed rapid extraction of the crucible from the furnace and enabled quenching of the material within 5 s of stopping the stirring. A free rotational bearing on top of the actuator prevented rotation of the crucible [29]. A356 was chosen as the matrix material for the compo-casting experimental work.

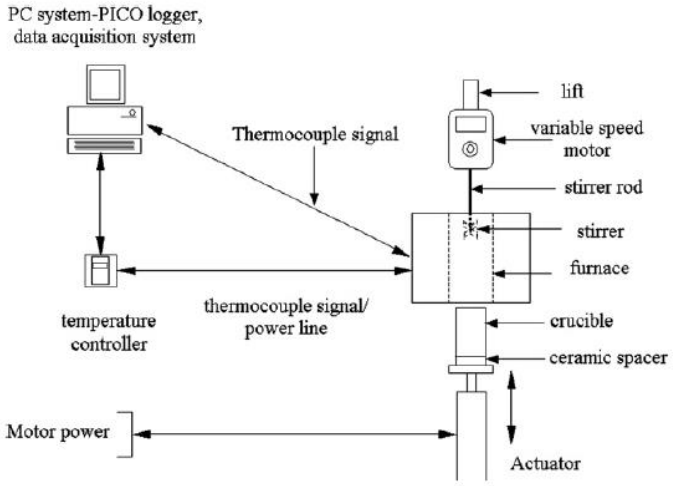

Fig. 2. Schematic of constructed compocaster.

At the start of each test, the 10% SiC was placed on the base of the crucible and cut to shape A356 ingot was placed on top of the SiC, to give a total height of 65 mm. The combination was then heated in the furnace to 650 °C and held for 30 min before the processing temperature was set and stirring commenced. This procedure, rather than introducing the particulate on top of the liquid or semi-solid metal, was found to provide consistently good particulate wettability. These tests were carried out in an inert nitrogen atmosphere. Two MMC ingot castings were fabricated in the liquid state at 650 °C with impeller rotational speeds of 200 and 300 rpm. For these tests the stirring period was set at 16 s. Six other ingot castings were fabricated via compocasting in the semi-solid state at 600 °C (approximately 0.3 fs) with stirring speeds of 200, 300, and 500 rpm. For the 200 rpm stirring speed, stirring times used were 1030 and 2335 s; for the 300 rpm stirring speed, stirring times used were 540 and 1030 s; and for the 500 rpm stirring speed, stirring times used were 120 and 540 s. The percentage of SiC at the specified height locations in the castings (indicated in Fig. lb) were calculated from image analysis (IA) of micrographs taken from sectioned samples at these locations. Percentage SiC values were recorded as the average percentage of SiC area from three representative images, each taken over a 0.45 mm2 sample area at the specified height locations.

3. Results

3.1. Computational results

3.1.1. Dispersion computational results

At stirring speeds above 300 rpm an excessively high vortex was created in the liquid metal analogue water fluid system. This indicated an upper processing bound for the liquid system. A lower processing bound presented itself for the glycerol/water system. At speeds below 200 rpm

the dispersion times were too long due to the higher viscos-ity of this system. The times taken to achieve uniform distributions of SiC at various stirring speeds within the two fluids, after commencement of stirring, are shown in Tables 1 and 2.

Table 1
Time to achieve a uniform 10% SiC particle distribution for different stirring speeds in water of viscosity 1 mPa s

Stirring speed (rpm)	Dispersion time (s)
100	170
150	28
200	16
250	15
300	14

Table 2
Time to achieve a uniform 10% SiC partucle distribution for different stirring speeds in glycerol/water solution of viscosity 300 mPa s

Stirring speed (rpm)	Dispersion time (s)
200	2335
250	1700
300	1030
400	720
500	540

These tables represent the times taken until a steady state distribution was achieved in the crucible. The steady state SiC distribution results at the various stirring speeds and locations in the crucible are presented in Figs. 3 and 4.

Fig. 3a—d shows the fraction of SiC against the radial distance from the central axis of the crucible for the water system. The key on the right of the graphs (P, Q, S, and T) indicates the height at which the radial fraction of SiC was computed, see Fig. lb. From Fig. 3a, it is can be seen that a significant fraction of SiC remains near the base of the crucible (location P), under the stirrer position.

However, Fig. 3b—d shows that at stirring speeds of 200 rpm and above, a relatively uniform fraction of SiC is present throughout the crucible. Fig. 4a—d represents the steady state distribution results for the glycerol/water system. A larger amount of particles can be seen under the stirrer position and at the wall for a stirring speed of 200 rpm in the glycerol/water system (Fig. 4a) compared with the water system (Fig. 3b). Larger resistance to particle dispersion was evident in the glycerol/water system due to its higher viscosity and density. At higher stirrer speeds in the glycerol/water system (Fig. 4b—d) a relatively uniform fraction of SiC was noted throughout the crucible.

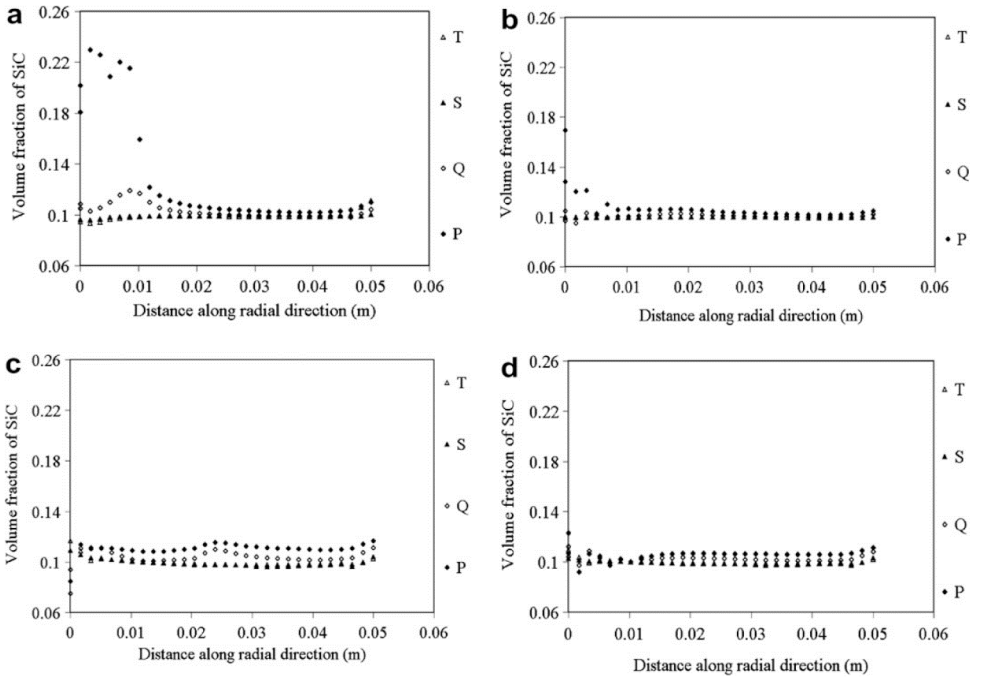

Fig. 3. Steady state distribution of SiC in water for stirring speeds of (a) 100 rpm, (b) 200 rpm, (c) 250 rpm, and (d) 300 rpm.

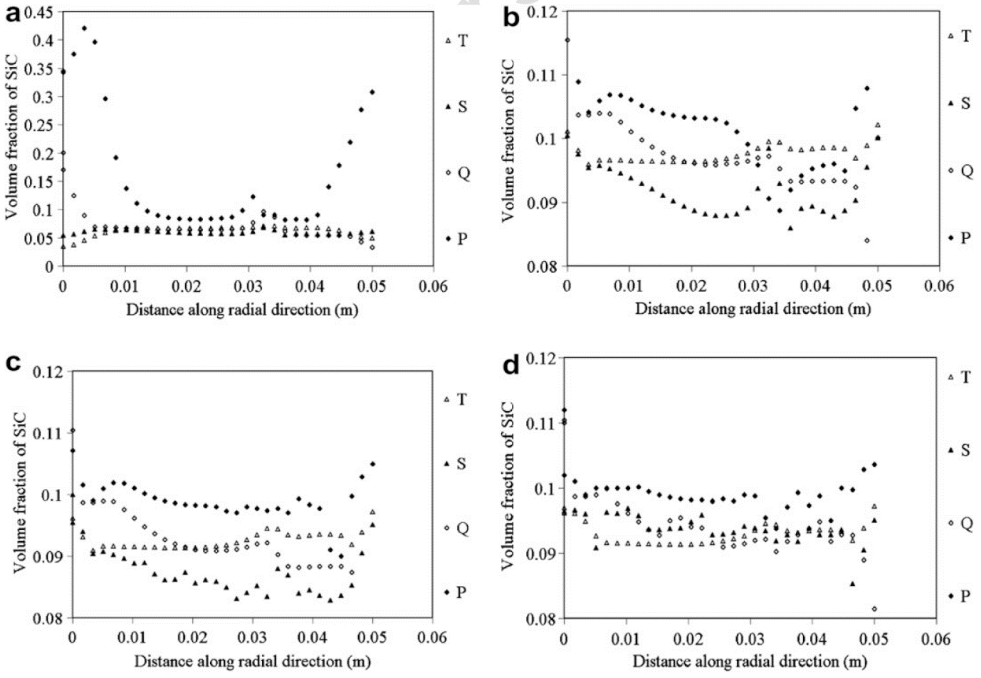

Fig. 4. Steady state distribution of SiC in glycerol/water for stirring speeds of (a) 200 rpm, (b) 300 rpm, (c) 400 rpm, and (d) 500 rpm.

3.1.2. Settling computational results

The settling simulations were started from a point of homogeneous distribution in the two fluids. Fig. 5 represents the volume fraction distribution at positions Q, S, and T during settling in the

water (Fig. 5a, c, and e) and the glycerol/water systems (Fig. 5b, d, and 0. After 60 s in the water system the volume fraction of SiC at the base of the crucible (Fig. 5a) approached the maximum packing fraction solid and little SiC remained in the upper part of the fluid (Fig. 5c and e). Settling took much longer, more than 3920 s, in the higher viscosity and density glycerol/ water system, see Fig. 5b, d, and f.

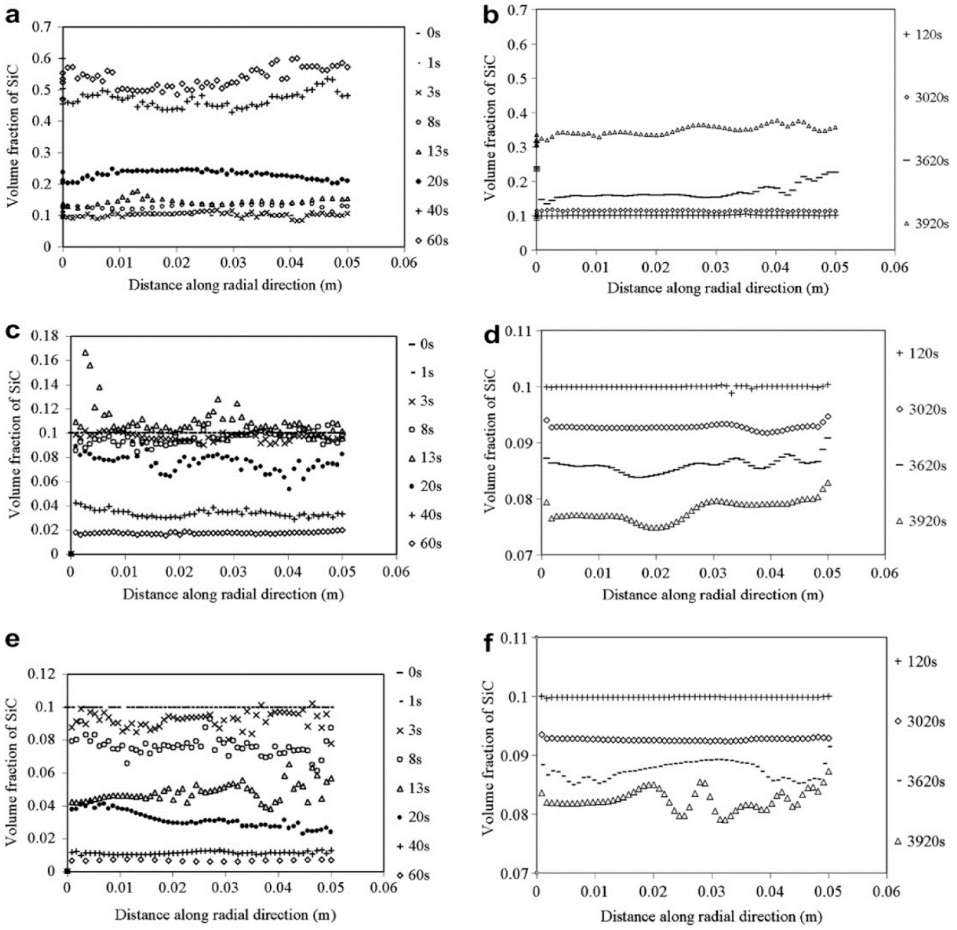

Fig. 5. Volume fraction of settled SiC as a function of radial distance in the water system: at positions (a) Q, (c) S, and (e) T; and the glycerol/water system: at positions (b) Q, (d) S, and (f) T.

The effect of different particle sizes (13, 30, and 100 μm) on settling rate was also examined. Fig. 6 shows the fractions of SiC during settling along a vertical plane in the fluid situated 8.5 mm from the outer wall. As expected from Stoke's law, the smaller diameter particles were seen to settle more slowly than the larger diameter particles.

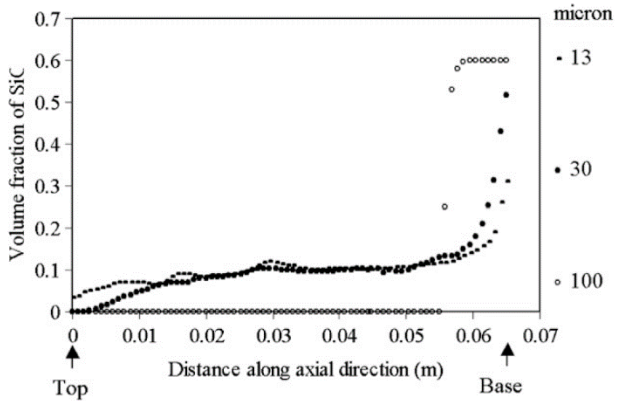

Fig. 6. Effect of particle size 9 min after the commencement of settling in a uniformly mixed water–10% SiC system.

3.2. Analogue results

3.2.1. Dispersion analogue results

Good correlation between the computational simulation (Tables 1 and 2) and analogue dispersion results was noted. Fig. 7a and b presents a comparison between the computational and analogue results in the two fluid systems. These figures suggest that for quick dispersion of SiC, a minimum stirring speed of 200 rpm should be used for liquid state processing and 300 rpm for the higher viscosity fluid system. Stirring speeds greater than 300 rpm generated excessively large vortices in both fluid systems at the fluid surface.

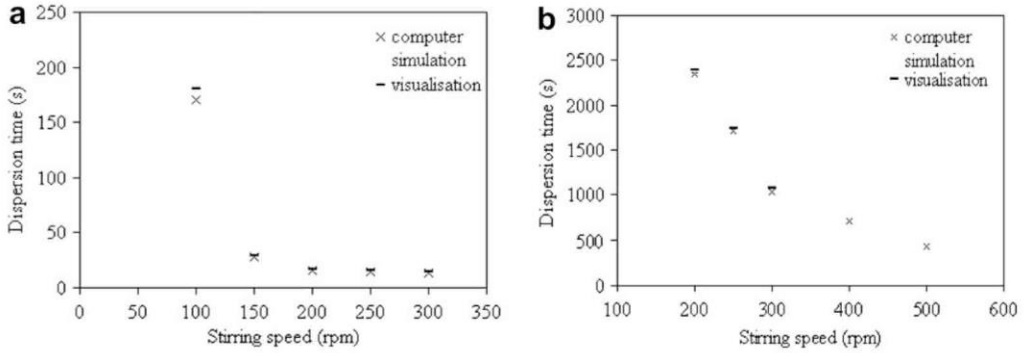

Fig. 7. Dispersion times for 10% SiC particles at various stirring speeds in (a) water and (b) glycerol/water solution.

3.2.2. Settling analogue results

Computational simulation and the analogue test results for settling rate also agreed well. In all cases, particulate settling times measured were independent of the stirring speed used to obtain the initial homogeneous distribution. Approximately 90% of all particles settled within 60 s in water and complete settling was recorded after approximately 180 s. The time at which particulate settling occurred in the glycerol/water mixtures was clearly evident from the emergence a transparent layer, absent of SiC particles, at the top of the mixture. For all glycerol/water mixtures a uniform dispersion of SiC remained for approximately 1 h, and complete particulate settling only occurred after 20 h.

3.3. MMC fabrication results

The average volume fraction of SiC at locations Q, S, and T was determined from image analysis (IA) of micro-graphs taken from sectioned samples at these locations. These volume fractions of SiC measured from the MMC disperiosn experiments are shown in Figs. 8 and 9, for the lower and higher viscosity systems, respectively. The computational results are also compared to the experimental results for the liquid system dispersion in Fig. 8 and settling in Fig. 10. As the models presented above do not account for thixotropic type fluid behaviour no such coma-prison is presented with the compocasting dispersion results which are shown in Fig. 9. However, as discussed in Section 2, a comparison may be made between the model and MMC fabrication settling results for semi-solid state processing. These results are presented in Fig. 11. A uniform distribution of SiC through the castings was judged to have occurred where the SiC percentage at the three locations was similar in level.

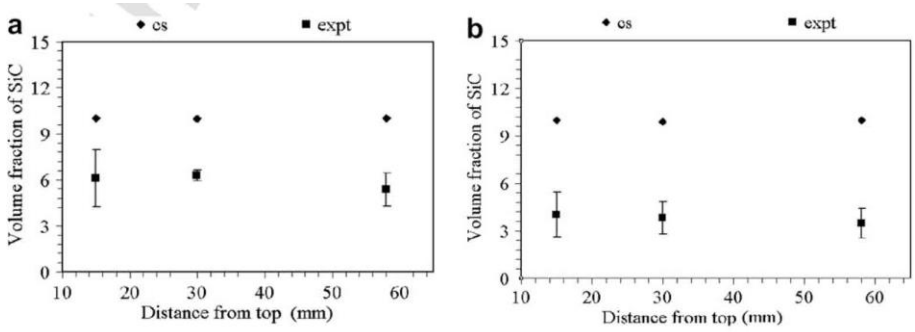

Fig. 8. Comparison of computer simulation and MMC fabrication experimental results for the volume fraction of SiC particles. Liquid state experiment processing parameters for stirring speed and time were: (a) 200 rpm, 16 s; and (b) 300 rpm, 16 s.

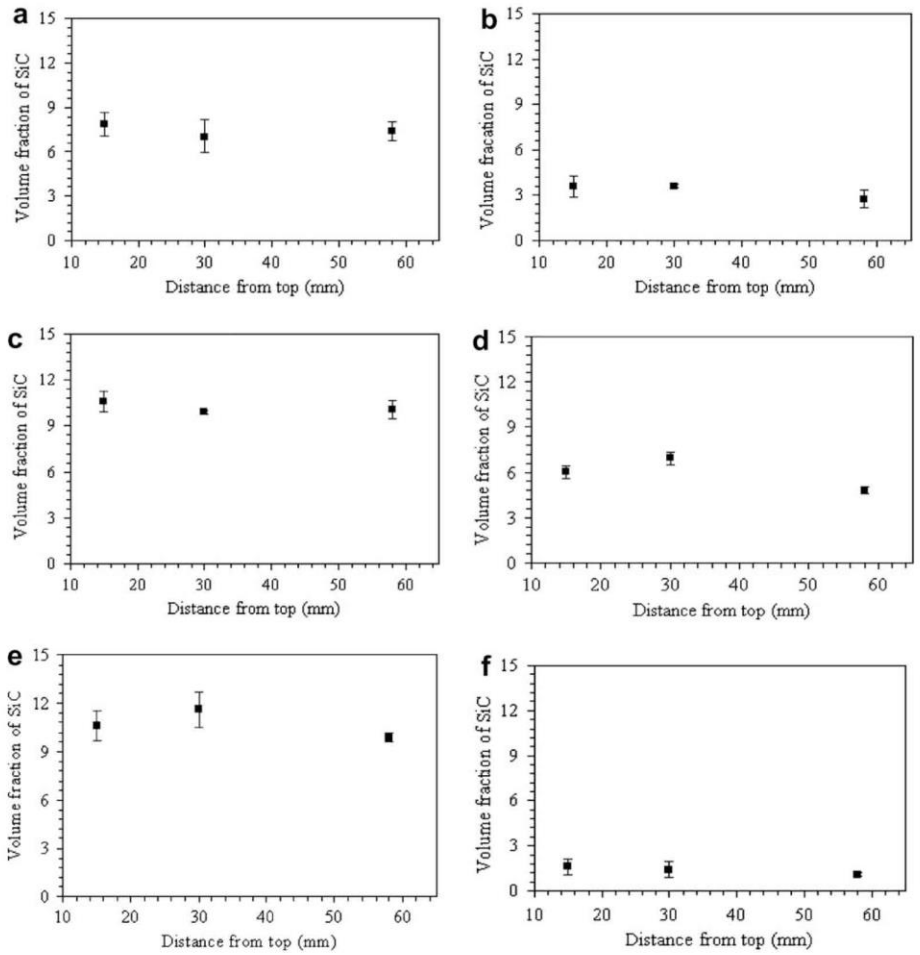

Fig. 9. Comparison of computer simulation and MMC fabrication experimental results for the volume fraction of SiC particles. Semi-solid state experiment processing parameters for stirring speed and time were: (a) 200 rpm, 2335 s; (b) 200 rpm, 1030 s; (c) 300 rpm, 1030 s; (d) 300 rpm, 540 s; (e) 500 rpm, 540 s; and (f) 500 rpm, 120 s.

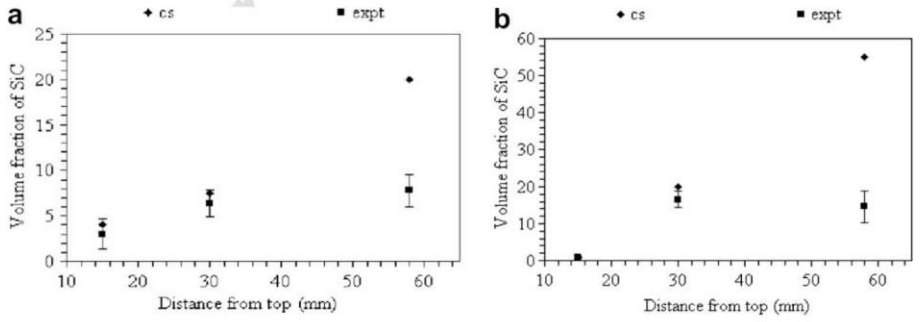

Fig. 10. Comparison of the volume fraction SiC determined from computational simulation and quenched compocastings (a) 20 s, and (b) 60 s after stirring was stopped. Before settling, uniform particulate distribution was achieved in the liquid system with a 200 rpm stirring speed applied for 16 s.

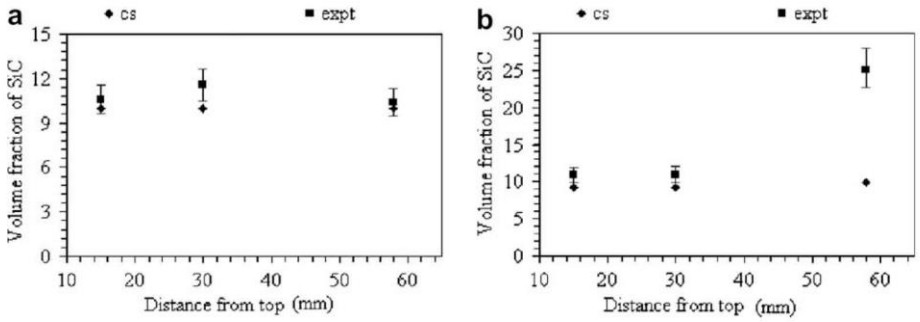

Fig. 11. Comparison of the volume fraction SiC determined from computational simulation and quenched compocastings (a) 120 s, and (b) 3020 s after stirring was stopped. Before settling, uniform particulate distribution was achieved in the semi-solid system with a 500 rpm stirring speed applied for 540 s.

4. Discussion

4.1. Computational and analogue simulations

A measure of the degree of suspension that is often used in the literature is the quantity of particulate remaining on the base of the vessel [30]. Experimental results from Rohatgi et al. examined the homogeneity of SiC distributions during stirring in water—SiC mixtures [22]. According to their work, the minimum speed required for a completely homogeneous suspension of SiC in water was found to be in the range 200-300 rpm. This agrees well with the results found in this work, see Fig. 3. For the higher viscos-ity glycerol/water system, a stirring speed of 300 rpm was found in the current work to be better suited to achieving a relatively uniform distribution, see Fig. 4. Dispersion times noted at the various stirring speeds in water are shown in Fig. 7a. From this figure it can be seen that the dispersion times at 100 rpm were determined as 170 and 180 s from the computer simulation and analogue experiments, respectively. Good correlation was again obtained between the analogue and computational simulation experiments for the higher viscosity glycerol/water fluid system. Fig. 7b shows that a much increased dispersion time of 2400 s at 200 rpm in this system.

From the results presented in previous work and above it is apparent that the stirring velocity has a significant effect on particle distribution in the water—SiC mixture [23]. These effects are dampened in the higher viscosity glycerol/water mixtures. Excessive vortex height that was recorded for some processing condition can result in air entrapment leading to internal voids and oxides within the casting which deteriorate the mechanical properties.

Non-reactive argon or nitrogen gas atmospheres mitigate the problems of oxide formation. However, these gases may also form pores when present within the SSM during solidification. Nevertheless, brute force has also been shown to provide a good method for incorporating particles in SSM [15]. With these points under consideration for batch MMC casting a production procedure is suggested as follows. The stirrer should produce strong currents in the bottom region of the SSM to encourage particle entrapment yet provide quiescent fluid surfaces to discourage gas entrapment. From the present work a stirring speed of 200 rpm and 300 rpm are suggested as the stirring speeds that can be used in the liquid at 1 mPa s and semi-solid states

at 300 mPa s, respectively, to promote particle dispersion yet guard against void entrapment. To obtain uniform particle distribution at these speeds periods of 16 s in the liquid state and 16 min in the higher viscosity fluid are required, see Fig. 7. It is therefore further suggested that, for higher production rates, the uniform distribution should be obtained in the liquid state after which temperature should be lowered into the semi-solid state to retain the uniform particulate distribution long enough for the forming operation to take place.

4.2. Computational and compocasting distributions

Uniform particulate distributions were obtained through the crucible in the liquid MMC dispersion experiments, see Fig. 8. It can be seen, however, that the computational simulation and experimental results do not correspond well. The experimental results in this case were lower than the computational results. Factors that could lead to differences between these results include particle pushing during solidification, non-wetting, clustering and settling before quenching which took up to 5 s [14,31,32]. These potential factors are discussed below.

Particle pushing by the solidification front has been recorded at undercoolings lower than 60 °C/s [33]. The critical velocity model presented by Stefanescu et al. was used to calculate the critical solidification front velocity [8,33]. This was found to be 4 pmts. The literature confirms that at solidification rates above this particle pushing would not be expected. Secondary phase particle pushing was not expected in this work as undercoolings of 100 °C/s and above were recorded. Previous examination of the compcasting cross-sectional micrographs also revealed a uniform distribution of particulate [29].

The wettability of SiC with liquid aluminium is low. This results in reduced fluid drag forces on the settled particles which could allow reduced settling rates in the compocastings when compared to the computational model results. However, in the present work extensive efforts and microstructural examinations were made to develop the system of casting (described in Section 2) so that particle wetting could be assured. As mentioned in Section 1 a number of workers have noted that particle clustering will tend to lead to an increased particle settling rate. No particulate clustering was evident in any of compocastings produced in this work [29]. This lack of clustering is believed to be due to the low volume fraction of re-inforcement and the stir-casting procedure used. The volume fraction percentage of particulate used in this work (10%) is at the low end of that which is currently used in practice [1]. The chances of reinforcement particle collisions would therefore be lower. In addition, the viscosities investigated (1 and 300 mPa s) were relatively low compared to industrial thixoforming process. At these lower stress levels, high stress concentrations which may force particulate together in other processes were not as prevalent [6].

Although settling is fast in the liquid system, after some analysis it can be shown that settling is not expected to have a large effect on the results. Stoke's law for particle settling can be used to express the terminal velocity of a falling particle in a homogeneously mixed system as fol-lows pf),g lows UT = c81, where x is the particle diameter (13 pm), pp is the particle density (3200

kg/m3), pf is the fluid density (1000 kg/m3), g is the gravitational constant (9.81 m/s2), and it/ is the viscosity of the fluid (1.3 mPa s and 390 mPa s in this case). Adjustment was required to the viscosity here to take account of the 10% particle con-tent [26]. This adjustment was automated in the CFD soft-ware. Using this equation terminal velocity for particles in the liquid system can be calculated as 0.16 mm/s. At this settling rate, only a small amount of settling is expected within a five second quench period. This settling value reduces to 0.0005 mm/s if the higher viscosity and density levels are used in the calculation. These settling rates com-pare well with those predicted by the computational model. Recalculating the settling rate with the density of aluminium (2700 kg/m3) for the liquid system gives a reduced settling value of 0.04 mm/s. With these settling rates in the liquid systems and within the five second quench period,the degree of settling cannot be expected to account for the results discrepancy in Fig. 8.

One other important possibile cause is the fact that suspensions in general and those examined in this work are shear thinning (pseudoplastic). Although the computational model does take account of the increased viscosity of the fluid, due to particulate content, the Newtonian model used does not predict pseudoplastic effects. Previous work has indicated Ostwald-De Waele power law exponents of between —0.6 and —0.99 in the aluimium alloy SiC composite system [34]. This appears to most reason-ably explain the reduced dispersion rates in the MMC fabrication experiments compared those found from the computational results.

During the compocasting process, Fig. 9a and b shows that a shear period slightly longer than 2335 s was required to produce a uniform distribution of SiC at a velocity of 200 rpm. At the higher stirring speed of 300 rpm, results in Fig. 9c and d, indicate that a lower shear period between 540 and 1030 s was required to produce a uniform distribution. At the highest stirring speed of 500 rpm, Fig. 9e and f shows that a shorter shear period between 120 and 540 s was required to produce a uniform distribution of SiC. The settling experiments were started from a point of uni-form particulate distributions. The processing parameters to achieve these uniform distributions were found from the dispersion experiments indicated above. Good correlation was found between the settling simulation results and the MMC liquid and semi-solid metal settling results, see Figs. 10 and 11. Interestingly, reasonable correlation was found for the semi-solid metal even for the higher period of 3020 s, see Fig. 11. The correlation between the computational and compocasting results agrees with the initial hypothesis that the Newtonian model can, with appropriate prior knowledge, be used for semi-solid fluids. Conditions for the use of such a model include restrictions to very low shear rate and limited periods. Prior experimental work to determine appropriate viscosity values, shear rates and periods would be needed to apply such a model to other settling conditions.

5. Conclusions

Speeds of 200 rpm for the lower viscosity system and 300 rpm for the higher viscosity system were determined as best in order to produce a uniform distribution of SiC. These agitation speeds allowed particle dispersion without inducing turbulent flow or gas entrapment. At these speeds

uniform distributions should be obtained after 16 s in the water system and after 16 min in the glycerol/water system. Due to the fast dispersion that occurs in the liquid state and slow settling in the semi-solid state, a processing regime can be devised to produce MMC parts. This would involve agitation in the liquid state to obtain a uniform particulate distribution, followed by reduction in temperature of the material into the semi-solid state to slow the settling of the particulate, and followed by laminar filling during forming of the MMC to shape. Results indicate that under certain well defined conditions, a Newtonian viscosity value can be used to predict particle settling during semi-solid MMC production. This would not hold true for particle dispersion which occurs at higher shear rates and therefore requires a more developed thixotropic type of fluid model. Reduced particle size was seen to result in a significant increase in settling times in accordance with Stoke's Law. However, increased dispersion times would also be expected with smaller particles sizes. For accuracy these models should also take account of parameter changes though the semi-solid regime such as shear rate, material densities, particulate shape, and particulate surface energy changes. The effect of these and other parameters on viscosity development in particular need to be investigated further to allow for a fuller knowledge of this process.

References

[1] Miracle DB. Metal matrix composites — from science to technology significance. Compos Sci Technol 2005;65:2526-40.

[2] Krishan BP, Surappa MK, Rohatgi PK. The UPAL process: a direct method of preparing cast aluminium alloy-graphite particle compos-ite. J Mater Sci 1981;16:1209-16.

[3] Hamilton R, Dashwood R, Zhu Z, Lee P. Direct semi-solid forming of a powder sical pmmc: flow analysis. Composites A 2003;34:333-9.

[4] Chen G, Jiang L, Zhang Q, Wu G, Luan B. The thermal expansion and mechanical properties of high reinforcement content SiCp-Al composites fabricated by squeeze casting technology. Composites A 2003;34:1023-7.

[5] Junyou L, Shiben W, Zhongliang S, Geying A. A new process for the fabrication of in situ particle reinforced metal matrix composites. J Mater Process Technol 1997;63:354-7.

[6] Cavaliere P. Isothermal forging of aa2618 reinforced with 20% of alumina particles. Composites A 2004;35:619-29.

[7] Evangelista E, Cerri E, Cavaliere P. Mechanical properties of an heat treated particle reinforced thixocast composite. In Chiarmetta GL, Rosso M, editors. Proceedings of the sixth international conference on the semi-solid processing of alloys and composites, Polytechnic di Turino, Turin, Italy, 27th-29th September 2000. p. 343-7.

[8] Dashwood RJ, Youssef YM, Lee PD. Effect of clustering on particle pushing and solidification behaviour in tib reinforced aluminium pmmcs. Composites A 2005;36:747-63.

[9] Lin CB, Ma CL, Chung YW. Microstructure of A380-SiCp compos-ites for die casting. J Mater Process Technol 1998;84:236-46.

[10] Geiger GH, Doirier DR. Transport phenomena in metallurgy. Read-ing, MA: Addison-Wesley; 1973.
[11] Laffreniere S, Iron GA. Sedimentation during liquid processing of metal matrix composites. In: Boushard M, Tremblay P, editors. Proceedings of international symposium on production, refining, fabrication and recycling of light metals. Oxford: Pergamon Press; 1990.
[12] Stefanescu D, Catalina A, Sen S, Dhindaw B, Currer P. Melt convection effects on the critical velocity of particle engulfment. J Cryst Growth 1997;173:574-84.
[13] Kathiresan S, Prabu S, Karunamoorthy L, Mohan B. Influence of stirring speed and stirring time on distribution of particles in cast metal matrix composite. J Mater Process Technol 2006;171:268-73.
[14] Oh SY, Cornie JA, Russell KC. Wetting of ceramic particle with liquid aluminium alloys. Part II: study of wettability. Metall Trans A 1989;20:533-41.
[15] Cornie JA, Moon HK, Flemings MC. A review of semi-solid slurry processing of Al matrix composites. In: Masounave J, Hamel FG, editors. Fabrication of particulates reinforced metal composites. ASM International; 1992. p. 63–78.
[16] Surappa AK, Rohatgi PK. Preparation and properties of cast aluminium ceramic particle composites. J Mater Sci 1981;16:981.
[17] Hashim J, Looney L, Hashmi MSJ. The enhancement of wettability of SiC particles in cast aluminium matrix composites. JMater Process Technol 2001;119:329–35.
[18] Armenante PM, Nagamine EU. Effect of low off-bottom impeller clearance on the minimum agitation speed for complete suspension of solids in stirred tanks. Chem Eng Sci 1998;53:1757–75.
[19] Tims ML, Xu J, Nickodemus G, Dax FR. Computer based numerical analysis of semi-solid metal working. In: Kirkwood DH, Kapranos P, editors. Proceedings of the fourth international conference on the semi-solid processing of alloys and composites, University of Sheffield, England, 19th–21th June 1996. p. 120–5.
[20] Lloyd DJ. Particle reinforced aluminium and magnesium matrix composites. Int Mater Rev 1994;39:1–23.
[21] Mortensen A, Jin I. Solidification processing of metal matrix composites. Int Mater Rev 1992;37:101–28.
[22] Rohatgi PK, Sobczak J, Asthana R, Kim JK. Inhomogeneities in silicon carbide distribution in stirred liquids – a water model study for synthesis of composites. Mater Sci Eng A 1998;252:98–108.
[23] Naher S, Brabazon D, Looney L. Simulation of the stir casting process. J Mater Process Technol 2003;143–144:567–71.
[24] Andersson H, Odenberger P, Lundstrom TS. Experimental flow-front visualisation in compression moulding of smc. Composites A 2004;35:1125–34.
[25] Quaak CJ, Kool WH, Sue´ry M. Assessment of semi-solid state forming of Al MMCs. Part 1: rheology. AFS Trans 1995;30:421–6.
[26] Rhodes M. Particle technology. New York: Wiley; 1998.

[27] Brabazon D. Processing and properties of rheocast alloys, Ph.D. Thesis, UCD, Dublin, Ireland, October 2001.
[28] Flemings MC. Behaviour of metal alloys in the semi-solid state. Metall Trans A 1991;22:957–81.
[29] Naher S, Brabazon D, Looney L. Development and assessment of a new quick quench stir caster design for the production of metal matrix composites. J Mater Process Technol 2004;166:430–9.
[30] Chudacek MW. Relationships between solids suspension criteria, mechanism of suspension, tank geometry and scale-up parameters in stirred tanks. Ind Eng Chem Fundam 1986;25:391–401.
[31] Zhou W, Xu ZM. Casting of SiC reinforced metal matrix composites. J Mater Process Technol 1997;63:358–63.
[32] Rohatgi PK. Future directions in solidification of metal matrix composites. Key Eng Mater 1995;104–107:293–312.
[33] Byrnes M, Wilde G, Perepezko J. Particle–dentrite interaction during undercooled liquid solidification of metal matrix composities. J Non- Cryst Solids 1999;250–252:626–31.
[34] Mada M, Ajersch F. Viscosity measurements of a356-15squeezing flow viscometer. In: Brown SB, Flemings MC, editors. Proceedings of the second international conference on the semi-solid processing of alloys and composites, 10 June 1992. Cambridge, MA: MIT Press; 1992. p. 276.